Eur Biophys J (2005) 34: 1–12
DOI 10.1007/s00249-004-0433-0

ARTICLE

Frank Gabel

Protein dynamics in solution and powder measured by incoherent elastic neutron scattering: the influence of Q-range and energy resolution

Received: 21 March 2004 / Revised: 6 July 2004 / Accepted: 8 July 2004 / Published online: 16 September 2004

Abstract Incoherent elastic neutron scattering (IENS) has been widely used to measure intramolecular atomic mean square displacements (MSDs) of proteins in powder and in solution. The instrumental energy resolution and the wave vector transfer (**Q**-range) determine, respectively, the time and length scales of observable motions. In order to investigate contributions of diffusive motions to MSDs measured by this method, we calculated the elastic intensity for several simple scattering functions. We showed that continuous translational diffusion contributes to MSDs in a **Q**-range where the energy width of the scattering function is of the order of the instrumental energy resolution. We discuss the choice of instruments adapted to focus on intramolecular motions in the presence of solvent or global macromolecular diffusion. The concepts developed are applied to interpret experimental data from H_2O- and D_2O-hydrated proteins. Finally, analogies between the Gaussian approximation in IENS and the Guinier approximation in small-angle scattering are discussed.

Keywords Energy resolution · Gaussian approximation · Incoherent elastic neutron scattering · Protein dynamics · Q-range

Introduction

Incoherent elastic neutron scattering (IENS) is a widely used method to measure atomic mean square displacements (MSDs) of hydrated protein powders, protein solutions and biological membranes on a pico- to nanosecond time scale (Smith 1991; Gabel et al. 2002). The method, also known as the ''elastic-window-method'', was introduced by Kollmar and Alefeld (1976). Its first application to biology concerned myoglobin intramolecular dynamics (Doster et al. 1989). Since then, the technique has been applied successfully to a number of important biological samples such as membranes (Ferrand et al. 1993), proteins in solution (Tehei et al. 2001) and powder form (Paciaroni et al. 2002), and more recently even to entire cells (Tehei et al. 2004). Owing to generally low neutron fluxes, IENS has often been preferred to incoherent quasi-elastic neutron scattering (IQNS). In this paper, we deal exclusively with applications of the IENS methodology to biological systems and not with the IQNS technique, whose importance for and application to biological problems have been treated elsewhere in detail (Fitter et al. 1996; Pérez et al. 1999).

In biological samples, thermal and cold neutron scattering cross-sections are dominated by the incoherent cross-section of hydrogen (H) (Sears 1984), which is also much larger than the scattering cross sections of its isotope deuterium (D). H–D exchange has therefore been used to highlight certain sample components, such as specific amino acids (Réat et al. 1998) or protein hydration water (Bellissent-Funel et al. 1996) in IENS or IQNS. Neglecting quantum effects and contributions of atoms other than H, the scattering function $S(\mathbf{Q},\omega)$ can be related to sample dynamics via a space-time Fourier transform of the hydrogen autocorrelation function (Van Hove 1954; Vineyard 1958). **Q** and ω represent, respectively, the amount (in units of $\hbar$) of momentum and energy exchanged by a neutron with the sample in a scattering event.

Models that have been used to describe atomic and molecular motions in biological samples include: a double-well potential (Doster et al. 1989), diffusion in a hard sphere (Volino and Dianoux 1980), continuous translational diffusion (Kneller and Smith 1994) or the Gaussian approximation for confined motions within a limited **Q**-range (Ferrand et al. 1993). Theoretical

F. Gabel
Institut de Biologie Structurale, 41 rue Jules Horowitz,
38027 Grenoble Cedex 1, France
E-mail: gabel@embl.de

Present address: F. Gabel
European Molecular Biology Laboratory,
Meyerhofstrasse 1, 69117 Heidelberg,
Germany

scattering functions $S(\mathbf{Q},\omega)$ could be measured directly only on a (hypothetical) instrument with infinitely good energy resolution, as described by a Dirac delta function. Real instruments, however, have finite energy resolutions and the measured intensity at ω contains weighted contributions from a range $\omega \pm d\omega$, where $d\omega$ is of the order of the instrumental energy resolution width. The instrumental resolution function is of particular importance in the case of diffusive motions, which are present in the following systems:

1. Macromolecules (e.g. proteins) in H_2O or D_2O solution (Tehei et al. 2001).
2. Samples containing ordinary water (H_2O) either in the form of hydration water or as the main solvent (Bellissent-Funel et al. 1996).
3. Membrane samples containing lipids (Lipowsky and Sackmann 1995).

Diffusion coefficients found in biological systems cover a range from $\sim 2.5\times10^{-9}$ m^2 s^{-1} (bulk water at ambient temperature) to $\sim 10^{-13}$ m^2 s^{-1} (lateral lipid diffusion in membranes, protein side-chain diffusion, self-diffusion of large globular proteins in crowded environments).

In this paper, we present calculations of the measured normalized elastic intensity in IENS as a function of the instrumental energy resolution width and $\mathbf{Q}$ for scattering functions $S(\mathbf{Q},\omega)$ that are used to describe biological systems in a simplified way. We use continuous translational motions to account for diffusive motions in the case of protein solutions and a more elaborate law in the case of hydrated protein powders. We investigate the contributions of the diffusive motions to MSDs and discuss those conditions under which instruments are apt to focus on intramolecular motions.

Theory

Real instruments have finite energy resolution functions and the measured scattering function $S_{\mathrm{meas}}(\mathbf{Q},\omega)$ represents a convolution of the theoretical $S(\mathbf{Q},\omega)$ with the instrumental energy resolution, $R(\omega)$:

$$S_{\mathrm{meas}}(\mathbf{Q},\omega) = R(\omega) \otimes S(\mathbf{Q},\omega) = \int_{-\infty}^{+\infty} S(\mathbf{Q},\omega')\, R(\omega-\omega')\, d\omega' \quad (1)$$

In the special case of elastic scattering, the convolution product of the instrumental resolution function and the theoretical scattering function has to be evaluated at $\omega = 0$ to obtain the measured elastic intensity (EI):

$$S_{\mathrm{meas}}(\mathbf{Q},0) = \int_{-\infty}^{+\infty} S(\mathbf{Q},\omega') R(0-\omega')\, d\omega' \quad (2)$$

Typical shapes of instrumental resolution functions are Gaussian, Lorentzian or triangular. Triangular resolution shapes result for some chopper-controlled time-of-flight instruments, whereas Gaussian and Lorentzian resolution functions are found for backscattering instruments and also for some time-of-flight instruments. For an overview of instrumental resolutions, see, for example, Bée (1988) or Frick and Farago (2002).

For convenience, we used normalized resolution functions:

$$\int_{-\infty}^{+\infty} R(\omega)\, d\omega = 1 \quad (3)$$

The different resolution functions can then be written in the following forms:

1. Lorentzian:

$$R(\omega) = \frac{1}{\pi}\frac{\Gamma_{\mathrm{Lor}}}{\omega^2 + \Gamma_{\mathrm{Lor}}^2} \quad (4)$$

where Γ_{Lor} is the resolution half-width at half-maximum (HWHM).

2. Gaussian:

$$R(\omega) = \frac{1}{\sigma\sqrt{2\pi}} \exp\left(-\frac{\omega^2}{2\sigma^2}\right) \quad (5)$$

with HWHM $\Gamma_{\mathrm{Gauss}} = \sqrt{2\ln 2}\sigma$.

3. Triangular:

$$R(\omega) = \frac{1}{(\omega*)^2}|\omega - \omega*|, \qquad |\omega| \leqslant |\omega*| \quad (6)$$

$$R(\omega) = 0, \qquad |\omega| > |\omega*| \quad (7)$$

where $\omega*/2$ is the HWHM of the resolution function.

The calculations in the next sections assume $\mathbf{Q}$-independent resolution functions, even though several instruments (notably time-of-flight spectrometers) have $\mathbf{Q}$-dependent resolution functions (Frick and Farago 2002). It is, however, possible to generalize our results to $\mathbf{Q}$-dependent resolution functions when the instrumental resolution shape is known as a function of $\mathbf{Q}$.

Results and discussion

In the following, we consider the incoherent H cross-section as dominant with respect to all other atomic cross-sections (coherent as well as incoherent), such that $S(\mathbf{Q},\omega)$ stands for $S_{\mathrm{incoh,H}}(\mathbf{Q},\omega)$.

Pure continuous translational diffusion

Continuous translational diffusion is a good approximation for the motion of bulk water and macromole-

cules in dilute solutions, provided the **Q**-values are not too large (i.e. focusing on large length scales).

The theoretical scattering function of continuous translational diffusion is given by a single, **Q**-dependent, Lorentzian function (Vineyard 1958):

$$S(\mathbf{Q},\omega) = \frac{1}{\pi}\frac{DQ^2}{\omega^2 + (DQ^2)^2} \tag{8}$$

where D is the translational self-diffusion coefficient given by the Einstein relation ($D = k_B T/6\pi\eta$r, where r is the hydrodynamic radius of the particle and η the viscosity of the solvent). The HWHM Γ_{diff} of Eq. (8) is given by:

$$\Gamma_{\text{diff}} = DQ^2 \tag{9}$$

Convolution with a Lorentzian resolution function

The measured EI of a continuous translational diffusion on an instrument with a Lorentzian energy resolution is given by the convolution of Eqs. (4) and (8) evaluated at $\omega = 0$ and yields (Gradshteyn and Ryzhik 1965):

$$S_{\text{meas}}(\mathbf{Q},0) = \left(1 + yQ^2\right)^{-1}, \qquad y = \frac{D}{\Gamma_{\text{Lor}}} \tag{10}$$

where we have used the convenient normalization $S_{\text{meas}}(\mathbf{Q} = 0,0) = 1$. Equation (10) shows that the EI of continuous translational diffusive motions as a function of **Q** is very sensitive to the ratio of the HWHM Γ_{diff} of the diffusive scattering function (Eq. 8) and the HWHM Γ_{Lor} of the Lorentzian energy resolution (Eq. 4). The normalized EI (Eq. 10) and its natural logarithm are traced for several ratios y as a function of Q^2 in Fig. 1a and Fig. 1b, respectively.

The different values of y were calculated for translational diffusion coefficients expressed in $\text{Å}^2\ \text{s}^{-1}$ and instrumental resolution HWHMs expressed in frequency units (s^{-1}) (with 1 μeV corresponding to $1.52\times10^9\ \text{s}^{-1}$); see Table 1.

As an example, bulk water ($D = 2.5 \times 10^{-9}\ \text{m}^2\ \text{s}^{-1} = 2.5\times10^{11}\ \text{Å}^2\ \text{s}^{-1}$) measured on an instrument with an energy resolution HWHM of 5 μeV

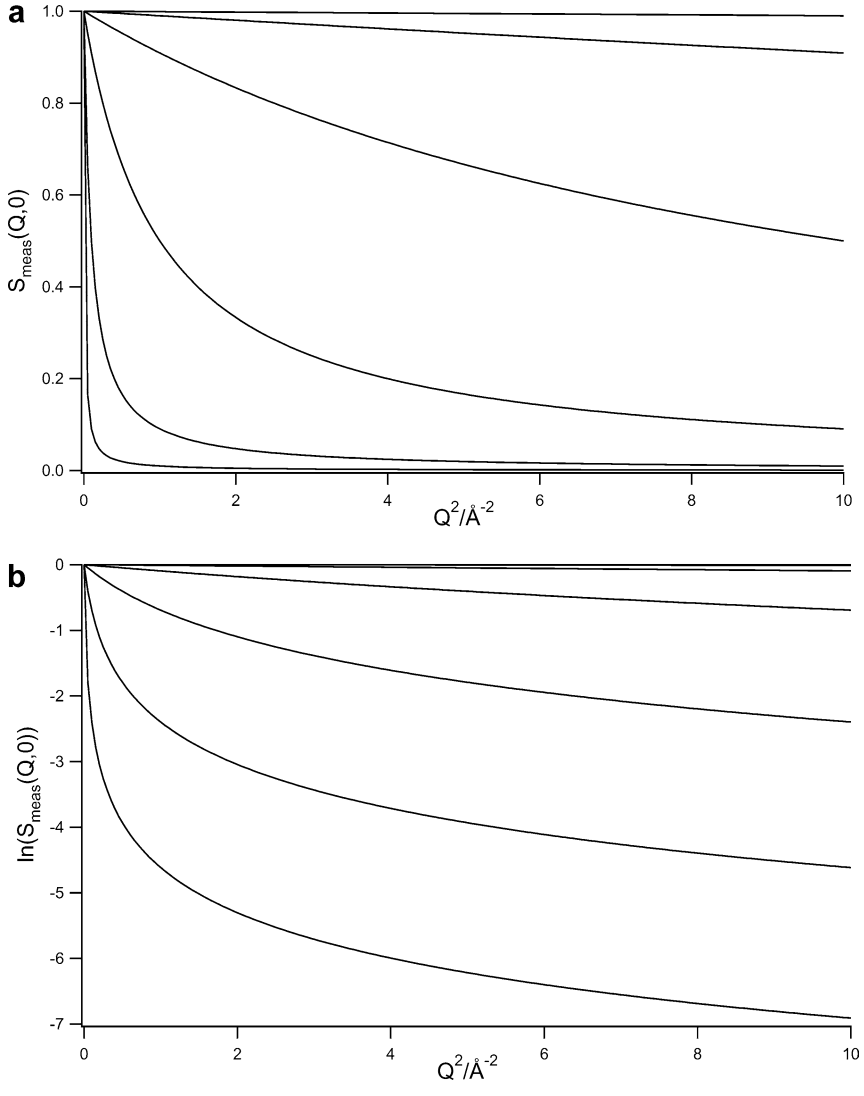

Fig. 1 Normalized EI and its logarithm for continuous translational diffusive motions as a function of Q^2 as measured by an instrument with a Lorentzian-shaped energy resolution. The curves were obtained from Eq. (10) for different values of $y = D/\Gamma_{\text{Lor}}$. *From top to bottom*: $y = 0.001$, 0.01, 0.1, 1, 10 and 100

Table 1 Values of $y = D/\Gamma_{Lor}$ (Eq. 10) for several macromolecular translational diffusion coefficients as well as bulk water for three instrumental resolution HWHMs

	5×10^{-13} m^2 s^{-1}	5×10^{-12} m^2 s^{-1}	5×10^{-11} m^2 s^{-1}	2.5×10^{-9} m^2 s^{-1}
0.5 μeV	0.066	0.66	6.6	330
5 μeV	0.0066	0.066	0.66	33
50 μeV	0.00066	0.0066	0.066	3.3

($=7.6\times10^9$ s^{-1}) corresponds to $y = 33$. Note that the same y-value can be realized for several D–Γ_{Lor} combinations. For example, measuring a translational diffusive motion with a tenfold increased diffusion coefficient on an instrument with a tenfold broadened resolution HWHM leaves y unchanged. Figure 1a and Fig. 1b illustrate the loss of the EI with increasing **Q**-values (corresponding to smaller distances in real space) with respect to the maximum normalized intensity, which is, theoretically, obtained at $\mathbf{Q} = 0$.

Three regimes can be distinguished for continuous translational diffusive motions:

1. The HWHM of the Lorentzian associated with the diffusive motions is much larger than the HWHM of the instrumental resolution ($y > > 1$): the elastic intensity decreases very quickly as the **Q**-values increase. At moderate **Q**-values ($Q > 1$–2 Å^{-1}), the elastic intensity scattered by atoms described by pure continuous translational diffusion is very close to 0 and can be considered as a negligible background with respect to the elastic intensity from different confined atoms of the sample having MSDs of the order of ~1 Å^2. If the continuous translational diffusion is superimposed on other motions for a single atom, it acts like an attenuating factor.
2. The HWHM of the Lorentzian associated with the diffusive motions is much narrower than the HWHM of the instrumental resolution ($y < < 1$): the elastic intensity decreases very slowly as the **Q**-values increase and can be considered as a constant. This reflects the fact that the Fourier transform of a point in real space (represented by a Dirac delta peak) is a constant in **Q**-space. Very slow diffusion of atoms of this category does not contribute to measured MSDs of confined atoms being characterized by MSDs of the order of ~1 Å^2.
3. The HWHM of the Lorentzian associated with the diffusive motions is of the order of the HWHM of the instrumental resolution ($y \approx 1$): the elastic intensity varies strongly over a wide range of **Q** and contributes notably to MSDs measured by methods using the **Q**-dependence of the elastic intensity.

Convolution with a Gaussian resolution function

The measured EI in this case is given by the convolution of Eqs. (8) and (5) at $\omega = 0$ and can be solved using the error function (Gradshteyn and Ryzhik 1965):

$$\mathrm{Erfc}(z) = 1 - \Phi(z) \tag{11}$$

where $\Phi(z)$ is the Fresnel integral defined by:

$$\Phi(z) = \frac{2}{\sqrt{\pi}} \int_0^z \mathrm{e}^{-t^2} \mathrm{d}t \tag{12}$$

After normalization [$S_{meas}(\mathbf{Q} = 0,0) = 1$], one obtains:

$$S_{meas}(\mathbf{Q}, 0) = \exp(z^2) \times \mathrm{Erfc}(z) \tag{13}$$

with:

$$z = \frac{DQ^2}{\sqrt{2}\sigma} = \frac{D\sqrt{\ln 2}}{\Gamma_{Gauss}} Q^2 \tag{14}$$

Equation (13) underlines that, here again, the EI is strongly sensitive to the ratio of the HWHM of the diffusive scattering function Γ_{Diff} and the Gaussian energy resolution Γ_{Gauss}. Note that, in contrast to a Lorentzian resolution shape, a factor $\sqrt{\ln 2}$ is contained in the crucial ratio z.

Convolution with a triangular resolution function

The measured EI is obtained by analogy to the two other cases by the convolution product of Eqs. (6) and (8). After normalization ($S_{meas}(\mathbf{Q} = 0,0) = 1$), one obtains (Volino et al. 1975):

$$S_{meas}(\mathbf{Q}, 0) = \frac{1}{\pi}\left[2 \times \arctan\left(\frac{\omega*}{DQ^2}\right) - \frac{DQ^2}{\omega*} \ln\left(1 + \left(\frac{\omega*}{DQ^2}\right)^2\right)\right] \tag{15}$$

Conclusions regarding resolution functions

The measured EI of continuous translational diffusion varies little between a Gaussian, Lorentzian and triangular resolution function (of the same HWHMs), as was checked by a graphical comparison of Eqs. (10), (13) and (15). This means that what was discussed under points 1–3 in the section "Convolution with a Lorentzian resolution function" for a Lorentzian-shaped resolution function remains valid for a Gaussian and for a triangular resolution function. We therefore used the Lorentzian resolution function in the following sections because of its mathematical simplicity regarding convolution products.

Continuous translational motions combined with motions described by the Gaussian approximation

Macromolecules in solution

At low **Q**-values, internal macromolecular fluctuations $<u^2>$ can be described by a Gaussian approximation in the form of a Debye–Waller factor:

$$S_{\mathrm{meas}}(\mathbf{Q},\omega=0) \propto \exp\left(-\frac{1}{6}<u^2>Q^2\right) \tag{16}$$

We use the term "Gaussian approximation" for Eq. (16) and not in the classical sense referring to a Gaussian-shaped correlation function; see, for example, Boutin and Yip (1968). The notation of Eq. (16) follows Réat et al. (1998) with respect to the definition of $<u^2>$, which represents the full amplitude of the motion and not the displacement from an equilibrium position. Equation (16) is valid as long as $<u^2>Q^2 \leq 2$. In this case, $<u^2>$ can be obtained by linear regressions in plots tracing the logarithm of the EI as a function of Q^2. Owing to their analogy to the Guinier approximation in small-angle scattering, we refer to these plots as Guinier plots.

In order to describe motions in solution, we superimposed intramolecular motions with global continuous translational diffusion of the macromolecules and added a contribution from the continuous translational diffusion of solvent water molecules. An additional Debye–Waller factor for the water molecules was neglected since it has been shown to be very close to 1 at ambient temperature (Teixeira et al. 1985) and in order not to introduce another parameter which would have to be fitted. The combined theoretical scattering function including all motions is then given by:

$$S(\mathbf{Q},\omega) = p_1 \exp\left(-\frac{1}{6}\langle u^2\rangle Q^2\right)\frac{1}{\pi}\frac{D_1Q^2}{\omega^2+(D_1Q^2)^2} + p_2\frac{1}{\pi}\frac{D_2Q^2}{\omega^2+(D_2Q^2)^2} + B(Q,\omega) \tag{17}$$

The intramolecular thermal fluctuations described by the Gaussian approximation (Eq. 16) are resolution-independent due to their elastic nature. $B(\mathbf{Q},\omega)$ represents inelastic contributions – due to the intramolecular thermal fluctuations – which assure the proper normalization of Eq. (17) when integrated over all energies. We assume that these inelastic contributions have energies of some millielectronvolts (which is in agreement with experimental work; Doster and Cusack 1990) and lie outside the investigated instrumental energy resolutions of less than a few hundred microelectronvolts. Therefore, the only **Q**-dependence of the intramolecular thermal fluctuations is contained in the Gaussian expression in Eq. (17).

Neglecting coherent contributions and focusing only on incoherent scattering of H-atoms, p_1 and p_2 represent the fractions of H-atoms from macromolecules and from water molecules, respectively, with $p_1+p_2=1$. D_1 is the macromolecular self-diffusion coefficient and D_2 is the translational diffusion coefficient of water (which we assume to be constant at 2.5×10^{-9} m^2 s^{-1} at ambient temperature; Weast 1975). For a Lorentzian-shaped instrumental resolution function with the HWHM Γ_{Lor}, the measured normalized EI can be written in the following form (by analogy to Eq. 10):

$$S_{\mathrm{meas}}(\mathbf{Q},0) = p_1\exp\left(-\frac{1}{6}\langle u^2\rangle Q^2\right)\left(1+y_1Q^2\right)^{-1} + p_2\left(1+y_2Q^2\right)^{-1} \tag{18}$$

where $y_1=\frac{D_1}{\Gamma_{\mathrm{Lor}}}$, $y_2=\frac{D_2}{\Gamma_{\mathrm{Lor}}}$.

We used Eq. (18) as a basic equation to describe sample motions in the following sections, varying the individual parameters as a function of sample composition.

Macromolecules in D_2O In Fig. 2, the natural logarithm of Eq. (18) is traced as a function of Q^2, varying y_1, with constant parameters $p_1=1$, $p_2=0$ and $<u^2>=0.5$ Å^2.

The five curves are calculated based on all possible combinations of the protein self-diffusion coefficients of $D_1=5\times10^{-11}$ m^2 s^{-1}, 5×10^{-12} m^2 s^{-1} and 5×10^{-13} m^2 s^{-1} and the instrumental HWHM of 0.5, 5 and 50 μeV. As in Fig. 1b, the curves in Fig. 2 depend strongly on the ratio y_1. For $y_1<<1$ (large instrumental resolution width and/or small diffusion coefficient), the curves decrease slowly as a function of Q^2, whereas for $y_1>>1$ (small instrumental resolution width and/or large diffusion coefficient), the normalized intensities decrease rapidly as a function of Q^2. We chose two **Q**-ranges to extract MSDs by linear fits: 1 Å$^{-2}<Q^2<2$ Å^{-2} and 2 Å$^{-2}<Q^2<4$ Å^{-2}. The extracted MSDs are shown in Table 2.

Only in the case $y_1<<1$ are the MSDs extracted by these fits close to the intramolecular Gaussian MSDs $<u^2>=0.5$ Å^2 of the macromolecules. In all other cases, the MSDs contain contributions from the self-diffusion of the macromolecules. The results imply that to extract correctly intramolecular MSDs in aqueous solution by the "elastic-window method" requires a ratio $y_1<0.01$. To give a practical example, on an instrument with a HWHM of ~5 μeV, only internal MSDs of macromolecules possessing a self-diffusion coefficient smaller than $\sim10^{-13}$ m^2 s^{-1} can be reasonably extracted without "contamination" from the macromolecular self-diffusion. It is therefore not possible to separate intramolecular MSDs properly from global self-diffusion of small globular proteins in dilute solution which have self-diffusion coefficients of $\sim5\times10^{-11}$ m^2 s^{-1} (Creighton 1993). However, protein self-diffusion coefficients have been found to be reduced by about an order of magnitude at concentrations >100 mg mL^{-1} required for neutron experiments (Dwyer and Bloomfield 1993; Ellis 2001).

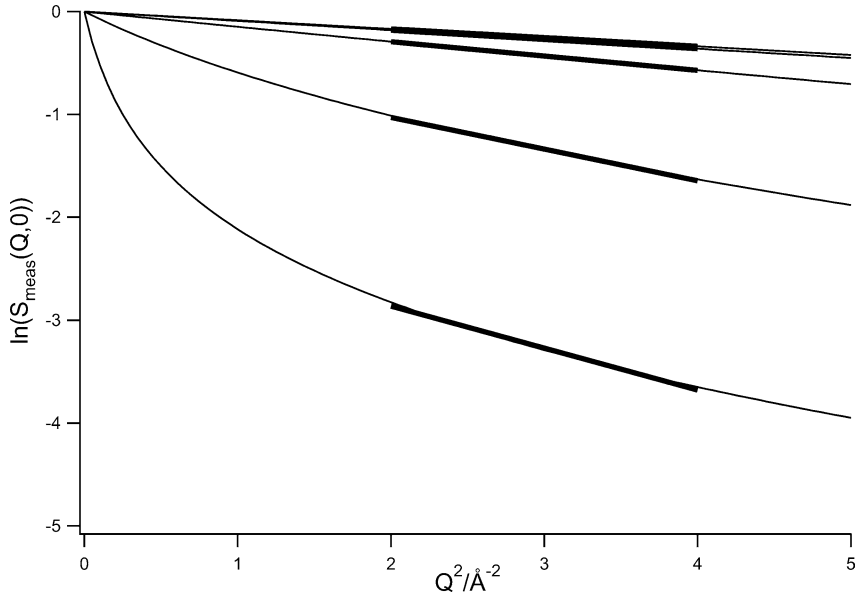

Fig. 2 Logarithms of the measured normalized EI for the model system "proteins in D_2O" (described by Eq. 18). The model parameters are $<u^2>=0.5$ Å^2, $p_1=1$, $p_2=0$, $D_1=5\times10^{-11}$, 5×10^{-12} and 5×10^{-13} m^2 s^{-1}, and $\Gamma_{Lor}=0.5$, 5 and 50 μeV. The y_1-values have been calculated for all possible combinations of D_1 and Γ_{Lor} (see also Table 2). *From top to bottom*: $y_1=0.00066$, 0.0066, 0.066, 0.66 and 6.6. The *thick lines* represent linear fits in the range 2 Å$^{-2}<Q^2<4$ Å^{-2} to extract MSDs (represented in Table 2). The line representing intramolecular motions in the absence of diffusive motions ($y_1=0$) coincides graphically with the uppermost curve ($y_1=0.00066$) and is not represented for reasons of clarity

Macromolecules in H_2O Tehei et al. (2001) measured MSDs in concentrated protein solutions (H_2O and D_2O) on IN13 (HWHM≈5 μeV) at the Institute Laue–Langevin (ILL). We use Eq. (18) with constant parameters $p_1=0.15$ and $p_2=0.85$, corresponding to a protein concentration of about 200 mg mL^{-1}, to describe the experimental situation in H_2O. As protein translational diffusion coefficients, we assume the three values already used in the section "Macromolecules in D_2O". In Fig. 3, we plot the natural logarithm of the measured normalized EI (Eq. 18) as a function of Q^2, varying y_1 and y_2 (i.e. the combination of the self-diffusion coefficients and the HWHM of the instrumental resolution), keeping $<u^2>=0.5$ Å^2 constant.

As in Fig. 2, we extract MSDs by linear regressions in two **Q**-ranges, 1 Å$^{-2}<Q^2<2$ Å^{-2} and 2 Å$^{-2}<Q^2<4$ Å^{-2}. The results, as well as the values y_1 and y_2 and their associated instrumental resolutions and diffusion coefficients, are given in Table 3. As in the case of proteins in D_2O, protein internal MSDs cannot be separated from the self-diffusion of the proteins if $y_1\approx1$.

An instrument with a narrow energy resolution (HWHM = 0.5 μeV) is not very suitable. Following results in D_2O (see section "Macromolecules in D_2O"), an instrument with a broad energy resolution (HWHM = 50 μeV) should be better fitted to focus on intramolecular motions. However, an instrumental HWHM of 50 μeV is of the order of the diffusion coefficient of H_2O molecules ($y_2\approx1$) and MSDs contain solvent contributions. Choosing the intermediate instrumental resolution width (HWHM = 5 μeV, $y_1=0.0066$, $y_2=33$) at a **Q**-range 2 Å$^{-2}<Q^2<4$ Å^{-2} yields the best results (0.65 Å^{-2} measured versus the theoretical 0.5 Å^{-2} for the protein internal MSDs). This is due to the fact that this energy resolution is large enough to comprise protein diffusive motions (for not too large self-diffusion coefficients; cf. case 1 in the section "Convolution with a Lorentzian resolution function") and at the same time, in combination with large **Q**-values, excludes contributions from H_2O. Comparing D_2O with H_2O measurements for an 5 μeV instrument in the large **Q**-range still leads to slight differences [$<u^2_{D2O}>=0.54$ Å^2 (Table 2) versus $<u^2_{H2O}>=0.65$ Å^2 (Table 3)], which converge only for very small protein self-diffusion coefficients ($D_1<5\times10^{-13}$ m^2 s^{-1}).

Table 2 MSD $<u^2>$ obtained by linear fits in the ranges 1 Å$^{-2}<Q^2<2$ Å^{-2} and 2 Å$^{-2}<Q^2<4$ Å^{-2} for the model system "proteins in D_2O" as a function of the ratio of the protein translational diffusion coefficients D_1 and the instrumental HWHM Γ_{Lor}, $y_1=D_1/\Gamma_{Lor}$ (Eq. 18). The model parameters are $<u^2>=0.5$ Å^2, $p_1=1$, $p_2=0$. The values y_1 are obtained by all possible combinations of $D_1=5\times10^{-11}$, 5×10^{-12} and 5×10^{-13} m^2 s^{-1} with the instrumental HWHM $\Gamma_{Lor}=0.5$, 5 and 50 μeV

y_1	6.6	0.66	0.066	0.0066	0.00066
$<u^2>$ (1–2 Å^{-2})	4.21 ± 0.06	2.51 ± 0.02	0.86 ± 0.00	0.54 ± 0.00	0.51 ± 0.00
$<u^2>$ (2–4 Å^{-2})	2.45 ± 0.03	1.85 ± 0.01	0.83 ± 0.00	0.54 ± 0.00	0.51 ± 0.00

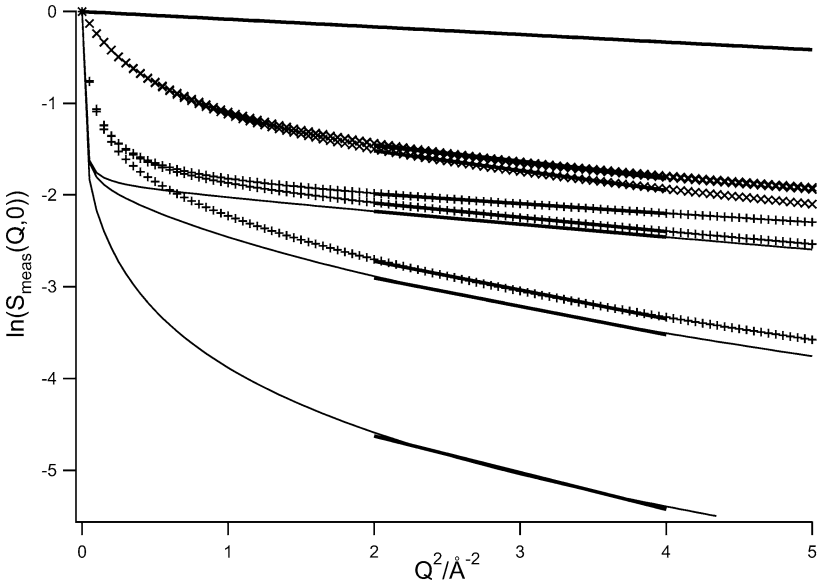

Fig. 3 Logarithms of the measured normalized EI for the model system "proteins in H_2O" (described by Eq. 18). The model parameters are $<u^2> = 0.5$ Å^2, $p_1 = 0.15$, $p_2 = 0.85$, $D_1 = 5\times10^{-11}$, 5×10^{-12} and 5×10^{-13} m^2 s^{-1}, $D_2 = 2.5\times10^{-9}$ m^2 s^{-1} and $\Gamma_{Lor} = 0.5$, 5 and 50 μeV. The curves are grouped according to their y_2-value: $y_2 = 3.3$ (*crosses*), 33 (*plusses*) and 330 (*dashes*). Each group is subdivided into three branches, representing different y_1-values (cf. Table 3), in increasing order *from top to bottom* in each group. The single uppermost *straight thick line* represents the pure intramolecular motions $<u^2> = 0.5$ Å^2 without diffusive contributions ($y_1 = y_2 = 0$). The *thick lines* represent linear fits in the range 2 Å$^{-2} < Q^2 < 4$ Å^{-2} to extract MSDs (as shown in Table 3)

However, working with large proteins in concentrated solutions on a ~5 μeV instrument in a large **Q**-range (Tehei et al. 2001) represents the best choice when intramolecular motions are to be extracted by IENS.

Hydrated macromolecular powders

In hydrated amorphous macromolecular (protein, membrane) powders (less than about 0.5 g water per gram dry material), macromolecular translational self-diffusion is supposed to be suppressed, in contrast to the solution case (Pérez et al. 1999). Scattering functions, under these conditions, describe protein internal molecular motions and hydration water motions.

Protein powders hydrated in H_2O and D_2O Continuous translational diffusion, as used in the preceding sections to describe bulk water or proteins in solution, provides only a poor description of confined hydration water (Bellissent-Funel 2004). In the following, we apply a phenomenological model to interpret the data of hydrated human butyrylcholinesterase (HuBChE) powders lyophilized from a phosphate buffer (Gabel et al. 2004). Our results and interpretations underline some general effects of diffusive motions on the measured EI.

Figure 4 compares the logarithm of the measured EI of H_2O- and D_2O-hydrated HuBChE powders as a function of Q^2. The HWHM of the instrumental resolution (IN16 at ILL) was 0.5 μeV. Hydration degrees of both samples were identical (0.42 grams of water per gram of dry material). In the H_2O-hydrated sample, 56% of the total incoherent scattering cross-section was assigned to protein atoms and 44% to the hydration water, whereas protein atoms accounted for about 100% of the total incoherent scattering cross-section of the D_2O-hydrated sample. A **Q**-independent shift to lower intensities was observed for the H_2O-hydrated sample with respect to its D_2O-hydrated counterpart. Elastic intensities of both samples at 280 K were normalized to their respective elastic intensities at 20 K, assuring independence of the number of scattering atoms.

Table 3 MSDs $<u^2>$ obtained by linear fits in the ranges 1 Å$^{-2} < Q^2 < 2$ Å^{-2} and 2 Å$^{-2} < Q^2 < 4$ Å^{-2} for the model system "proteins in H_2O" as a function of the ratio of the protein translational diffusion coefficient D_1 and the instrumental HWHM Γ_{Lor}, $y_1 = D_1/\Gamma_{Lor}$, and the ratio of the solvent water translational diffusion coefficient and the instrumental HWHM, $y_2 = D_2/\Gamma_{Lor}$ (Eq. 18). The model parameters are $<u^2> = 0.5$ Å^2, $p_1 = 0.15$, $p_2 = 0.85$. The values y_1 and y_2 are obtained by all possible combinations of $D_1 = 5\times10^{-11}$, 5×10^{-12}, 5×10^{-13} m^2 s^{-1} and $D_2 = 2.5\times10^{-9}$ m^2 s^{-1} with the instrumental HWHM $\Gamma_{Lor} = 0.5$, 5 and 50 μeV

Γ/y_2	0.5 μeV/330			5 μeV/33			50 μeV/3.3		
y_1	6.6	0.66	0.066	0.66	0.066	0.0066	0.066	0.0066	0.00066
$<u^2>$ (1–2 Å^{-2})	4.20 ± 0.07	2.55 ± 0.02	0.91 ± 0.00	2.82 ± 0.04	1.26 ± 0.02	0.95 ± 0.02	2.25 ± 0.04	2.04 ± 0.04	2.00 ± 0.00
$<u^2>$ (2–4 Å^{-2})	2.40 ± 0.03	1.85 ± 0.01	0.85 ± 0.00	1.88 ± 0.02	0.93 ± 0.00	**0.65 ± 0.00**	1.29 ± 0.01	1.08 ± 0.01	1.06 ± 0.00

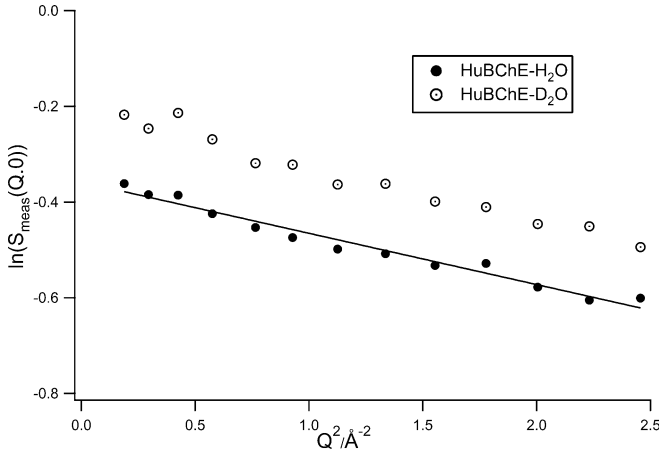

Fig. 4 Logarithm of the measured EI on IN16 at 280 K (normalized to 20 K) of human butyrylcholinesterase (HuBChE) hydrated in H_2O and D_2O (adapted from Gabel et al. 2004). The logarithm of Eq. (20) is traced for HuBChE-H_2O. $A = 0.82$ (extracted by fitting Eq. 20 to HuBChE-D_2O) as well as $p = 0.56$ (from Gabel et al. 2004) were kept fixed to extract $<u^2> = 0.64$ Å^2 and $\Gamma_{diff}/\Gamma_{Lor} = 0.84$ from the fit using the logarithm of Eq. (20)

The **Q**-independent intensity loss of the H_2O-hydrated sample with respect to its D_2O-hydrated counterpart suggests **Q**-independent diffusive motions of the hydration water (provided that internal protein dynamics does not depend on water isotopic effects). The presence of the shift at the lowest measured **Q**-value ($Q^2 = 0.19$ Å^{-2}) implies, owing to the reciprocity between **Q**-range and real space, long-range diffusive motions. However, attempts to fit the experimental data assuming that all hydration water molecules undergo continuous translational motions overestimated the shift between the H_2O-hydrated and the D_2O-hydrated samples (not shown). We therefore applied a phenomenological scattering function (Eq. 19) to the data, inspired by a jump-diffusion model presented by Teixeira et al. (1985). In this model, the HWHM of the scattering function increases at low **Q**-values, as for continuous translational diffusion, but levels off to a plateau value at higher **Q**-values:

$$S(\mathbf{Q},\omega) = Ap\exp\left(-\frac{1}{6}\langle u^2\rangle Q^2\right) + (1-p)\exp\left(-\frac{1}{6}\langle u^2\rangle Q^2\right)\frac{1}{\pi}\frac{\Gamma_{diff}}{\omega^2+\Gamma_{diff}^2} \quad (19)$$

The measured elastic intensity is given by convoluting Eq. (19) with Eq. (4):

$$S(\mathbf{Q},0) = Ap\exp\left(-\frac{1}{6}\langle u^2\rangle Q^2\right) + (1-p)\exp\left(-\frac{1}{6}\langle u^2\rangle Q^2\right)\left(1-\frac{\Gamma_{diff}}{\Gamma_{Lor}}\right)^{-1} \quad (20)$$

Equation (19) is based on the assumption that the HWHM Γ_{diff} associated with diffusion of the hydration water increases at **Q**-values smaller than $Q^2 = 0.19$ Å^{-2} and remains constant in the measured **Q**-range. p represents the total (incoherent) scattering cross-section due to the protein H population, while its complement, $1-p$, is assigned to the hydration water. A is a phenomenological factor that represents non-Gaussian contributions of the protein atoms (and possible multiple scattering effects). It was extracted by y-axis intersection of linear fits of the D_2O-hydrated sample data points (where $p = 1$). $<u^2>$ represent MSDs of motions described by the Gaussian approximation. These MSDs are assumed to be identical for protein atoms and hydration water, as suggested by the identical slope of H_2O- and a D_2O-hydrated sample intensities as a function of Q^2. A, p and $<u^2>$ being thus fixed, information can be obtained on Γ_{diff} by the shift between H_2O- and D_2O-hydrated samples. Fitting the H_2O-hydrated sample gives $\Gamma_{diff}/\Gamma_{Lor} = 0.84$, i.e. $\Gamma_{diff} = 0.42$ μeV. An estimate of the continuous translational diffusion coefficient assumed to predominate at **Q**-values smaller than the smallest measured **Q**-value ($Q^2 = 0.19$ Å^{-2}) is obtained by evaluating Eq. (9) at $Q^2 = 0.19$ Å^{-2}, using $\Gamma_{diff} = 0.42$ μeV. The translational diffusion coefficient thus obtained, $D = 3.4\times10^{-11}$ m^2 s^{-1}, is ~30 times smaller than that of bulk water at 273 K (Bellissent-Funel 2004). It is situated in the lower range of literature data but compares well to diffusion coefficients published by Settles and Doster (1996), who found values from 2×10^{-11} m^2 s^{-1} to 1×10^{-10} m^2 s^{-1} at 320 K in myoglobin hydration water, and Bon et al. (2002), who found 5×10^{-11} m^2 s^{-1} at 300 K for water in lysozyme crystals.

We stress that the model used to interpret the experimental data is purely phenomenological and alternative interpretations, e.g. continuous translational diffusion of only a fraction of the hydration water or more complicated models, are possible. However, our phenomenological approach explains quantitatively the differences observed between H_2O- and D_2O-hydrated protein powders by Gabel et al. (2004), and leads to a hydration water diffusion coefficient that is situated in the range of literature values. Furthermore, the calculations reflect the general concept of the present article, i.e. the importance of the absolute value of the measured elastic intensities when diffusive motions of the order of the instrumental energy resolution are present. Using only slopes of linear fits in defined **Q**-ranges to extract MSDs may neglect important information.

Polydispersity of motions and other complications

Polydispersity of macromolecular motions and analogies to the Guinier approximation in small-angle scattering A major problem with the models chosen in the preceding sections is that they describe protein molecular motions as monodisperse, i.e. all protein atoms as dynamically equivalent. This is clearly wrong as has been shown, for example, by *B*-factors in X-ray measurements (Frauenfelder et al. 1979) or specific labelling in neutron

scattering experiments (Réat et al. 1998). IENS data have therefore been interpreted in terms of different dynamical populations by analogy to the Guinier approximation in small-angle scattering (SAS) (Réat et al. 1997).

In SAS, the scattered intensity of a single macromolecule is given by the square of the absolute value of the Fourier transform of the scattering particle (e.g. electrons in X-ray scattering and nuclei in neutron scattering) density distribution $\rho(\mathbf{r})$:

$$I(\mathbf{Q}) = A(\mathbf{Q})A^*(\mathbf{Q}) = |A(\mathbf{Q})|^2 = \left| \int \rho(\mathbf{r}) \exp(i\mathbf{Q} \times \mathbf{r}) \, \mathrm{d}^3\mathbf{r} \right|^2 \quad (21)$$

This expression is mathematically equivalent to the elastic incoherent structure factor (EISF), i.e. the time-independent part of the incoherent scattering of a single nucleus (Bée 1988):

$$\mathrm{EISF} = \left| \int p_\infty(\mathbf{R}) \exp(i\mathbf{Q} \times \mathbf{R}) \mathrm{d}^3\mathbf{R} \right|^2 \quad (22)$$

where the equilibrium distribution $p_\infty(\mathbf{R})$ at infinite time of the EISF in IENS corresponds to the spatial density distribution $\rho(\mathbf{r})$ in SAS.

Considering a dilute solution of monodisperse macromolecules in SAS, the measured intensity can be approximated, after averaging over all possible macromolecular rotational orientations, by the Guinier approximation (Guinier and Fournet 1955):

$$I(\mathbf{Q}) \propto \exp\left(-\frac{1}{3} R_g^2 Q^2\right) \quad (23)$$

where R_g is the radius of gyration of the macromolecules.

Whatever the shape of the particles, this approximation holds for the product:

$$R_g^2 Q^2 \leqslant 1 \quad (24)$$

Averaging a macromolecule over all possible orientations in SAS corresponds to a single dynamical population of atoms undergoing the same motions (i.e. being placed in identical potentials) oriented in different spatial directions in IENS. Equation (23) is mathematically analogous to the Gaussian approximation (Eq. 16). The fact that the MSD $<u^2>$ values in Eq. (16) are twice the squared radius of gyration, ${R_g}^2$, is a consequence of our definition of the MSDs in Eq. (16). In the framework of this formal analogy, results of IENS experiments can be interpreted in the light of results of SAS experiments of dilute solutions. For example, a polydisperse dilute solution of macromolecules can be likened to dynamically different atomic populations in an incoherent scattering experiment. However, the analogy is not perfect between the EI in IENS and the elastically scattered intensity in SAS, for two reasons:

1. The EI in IENS consists not only of the time-independent part, i.e. the EISF. It is "contaminated" by time-dependent contributions which are due to the finite instrumental energy resolution. This is inherent to IENS and there exists no direct analogy in SAS. Care has therefore to be taken when interpreting the EI in IENS experiments within the Gaussian approximation (Becker and Smith 2003). In order to estimate (in a simplified way) the corrections due to the instrumental resolution, we assume that the system returns to equilibrium by a single exponential dynamical process with a relaxation time τ. If the relaxation process is much slower than the instrumental time resolution, $\tau_{\mathrm{Lor}} = 1/\Gamma_{\mathrm{Lor}}$, i.e. $\tau_{\mathrm{Lor}} << \tau$, the EI is almost a constant function of **Q** and the extracted MSDs zero, as would be expected for a particle that stands still during the instrumental observation time. On the other hand, if the relaxation process is much faster than the instrumental time resolution ($\tau_{\mathrm{Lor}} >> \tau$), the measured EI is very well represented by the Gaussian approximation for confined motions. Throughout this Results and discussion section, we have neglected the time-dependent contribution to the EI and used the Gaussian approximation for intramolecular motions. Is this reasonable for macromolecules in solution and powder form? Or, in other words, how do typical relaxation times of the intramolecular motions compare to the instrumental resolutions used? Pérez et al. (1999) described the time-dependent contributions in the case of myoglobin and lysozyme in powder and in solution by a single relaxation process, i.e. by a single Lorentzian-shaped function. The authors found a maximum linear increase of its width of ~40% in solution and powder in the **Q**-range 0.2 $\mathrm{Å}^{-2} < Q^2 < 3$ $\mathrm{Å}^{-2}$ and correlation times of ~10 ps in powders and ~5 ps in solution. The instrumental energy HWHM used in this "Results and discussion" section, i.e. 0.5, 5 and 50 μeV, have corresponding observation times of ~650, 65 and 6.5 ps, respectively. This means that the instrument with the shortest observation time (6.5 ps) is sensitive to the time aspects of intramolecular motions, whereas the two instruments with longer observation times are less sensitive and should be privileged when interpreting IENS experiments by analogy to the Guinier approximation in SAS. Varying the instrumental energy resolution width has been applied recently to weakly scattering biological samples (Doster et al. 2003) and seems to be a promising IENS method in order to explore the different time scales of macromolecular dynamics.
2. When radii of gyration of homogeneous particles are measured in SAS experiments, large particles dominate strongly at small **Q**-values (Guinier and Fournet 1955). This is due to (1) the fact that the number of scatterers in a particle goes with the third power of the particle radius and (2) the fact that the spatial Fourier transform of large particles diminishes more rapidly with **Q** than the one from smaller particles.

For a polydisperse solution of geometrically similar particles, the extracted mean square radius of gyration, R_M^2, at $\mathbf{Q} \to 0$ is given by (Guinier and Fournet 1955):

$$R_M^2 = \frac{\sum_k p_k R_k^8}{\sum_k p_k R_k^6} \tag{25}$$

where p_k represent the proportions (by number) of the particles with radius R_k. In IENS experiments, point (2) is fulfilled since the Fourier transform of large amplitude (confined) motions decreases more rapidly than the Fourier transform of small amplitude (confined) motions. However, point (1) does not hold for IENS experiments since each nucleus scatters independently and large amplitude motions are disfavoured due to a "thinning out" of the scatterer's probability distribution in space with respect to small amplitude motions. One therefore has the MSDs $< u_M^2 >$ for $\mathbf{Q} \to 0$:

$$\langle u_M^2 \rangle = \sum_k p_k \langle u_k^2 \rangle \tag{26}$$

where the p_k represent the proportions (by number) of the different dynamical populations. Equations (25) and (26) are at the origin of restrictions concerning the interpretation of dynamical populations in IENS experiments in terms of a polydisperse solution in SAS. To illustrate the differences between both equations, we suppose a solution containing particles of two sizes, $R_2^2 = 2R_1^2$ (with $p_1 = p_2 = 1/2$), on the one hand, and two dynamical populations, ($p_1 = p_2 = 1/2$) with $\langle u_2^2 \rangle = 2\langle u_1^2 \rangle$ on the other, i.e. one population has twice the square radius of the other. With Eqs. (25) and (26), the mean square radius of gyration and the MSDs are then $R_M^2 = \frac{17}{18} R_2^2 \approx 0.94 R_2^2$ and $\langle u_M^2 \rangle = \frac{3}{4} \langle u_2^2 \rangle = 0.75 \langle u_2^2 \rangle$, respectively. As becomes evident, there is a notable difference between both cases. Calculating the mean radius of gyration by weight (i.e. for $p_1 = 0.74$ and $p_2 = 0.26$), leads to the result $R_M^2 \approx 0.87 R_2^2$, a value closer to the MSDs result of IENS but still notably different. In conclusion, in IENS experiments, large amplitude populations do not dominate to the same extent as they do in SAS experiments.

Rotational diffusion Macromolecular diffusion in a solvent is described more precisely when taking an additional rotational diffusion into account (Pérez et al. 1999). However, as has been shown by quasielastic neutron scattering in the case of lysozyme and myoglobin (Pérez et al. 1999), rather than changing qualitatively the diffusion process, the rotational diffusion coefficient, in a first approximation, adds up to the translational diffusion coefficient for sufficiently large **Q**-values. The resulting apparent diffusion coefficient is ~30% larger than the translational diffusion coefficient alone (Pérez et al. 1999). In the light of these experimental results, the calculations carried out in the present paper are qualitatively valid and may be adapted, taking this increase into account.

Solvent viscosity Since the viscosities of ordinary and heavy water differ by about 30% at 20 °C (Pérez et al. 1999; Weast 1975), the diffusion coefficient of solutes varies by the same percentage, owing to the Einstein relation. This difference has to be taken into account when internal MSDs of macromolecules dissolved in H_2O and D_2O are compared. In our case, the MSDs in Table 2 (macromolecules in D_2O) are decreased by up to ~10% (for $y_1 \approx 1$), but remain essentially unchanged for $y_1 << 1$.

Exchangeable protons Owing to exchangeable protons, the observable macromolecular populations are different when H_2O or D_2O is used as a solvent. In D_2O, ~10–20% of protein protons may exchange. Since these protons are often situated close to the protein surface, the exchange may influence extracted MSDs since surface protons may be dynamically different from interior (e.g. backbone) protons (Dellerue et al. 2001). In an extreme case, assuming exchangeable proton dynamics similar to hydration water dynamics, the population p_1 in Table 3 would simply decrease by ~20%, i.e. $p_1 = 0.13$, and leave the results essentially unchanged. The same is true for the other extreme case: exchangeable protons behave like non-exchangeable protons. However, care has to be taken when exchangeable proton dynamics is assumed to be situated between bulk water dynamics and non-exchangeable proton dynamics (Dellerue et al. 2001).

Overview and classification of existing neutron scattering instruments

Table 4 lists accessible energy resolution- and **Q**-ranges of some of the existing neutron scattering instruments (adapted from Frick and Farago 2002). It provides neutron users with the possibility of classifying instruments in the light of the results presented in this article. If both Gaussian motions and continuous translational

Table 4 Accessible energy resolution- and **Q**-ranges of several neutron scattering instruments available at different reactors and spallation sources (Frick and Farago 2002)

Instrument	Energy resolution HWHM (μeV)	**Q**-range ($Å^{-1}$)
IN10, ILL (France)	0.4–1.75	0.07–3.7
IN13, ILL (France)	4–8	0.7–5.2
IN16, ILL (France)	0.42–1	0.07–3.7
BSS Jülich (Germany)	0.5	0.07–2
NIST HFBS (USA)	0.45	0.1–1.8
FRM II (Germany) project	0.45	0.1–1.8
IRIS, ISIS (UK)	0.5–25	0.1–3.7
OSIRIS, ISIS (UK)	12.5	0.1–1.8
LAM-80ET, KENS (Japan)	0.6–2.8	0.1–1.8

diffusion are present in an investigated sample, the *y*-criterion (''Convolution with a Lorentzian resolution function'' section) permits a classification of instruments (taking into account their energy resolution width and accessible **Q**-range) as being adapted or not to focus on Gaussian intramolecular motions. [For example, the ILL instrument IN13, having an energy HWHM of about 5 μeV and a large **Q**-range, is one of the best-suited instruments to focus on internal protein dynamics in solution, whereas in the case of IN16 and IN10, owing to their small **Q**-values, contributions of protein global diffusion in solution are to be expected. OSIRIS and IRIS are, when operated at energy resolutions of several tens of microelectronvolts, well suited to focus on water dynamics or protein global diffusion in solution rather than on internal protein dynamics.] In the more general case of arbitrary diffusive motions being described by a combination of elastic and quasi-elastic components (e.g. as in the section ''Protein powders hydrated in H_2O and D_2O''), the capacity of a particular instrument to focus on Gaussian intramolecular motions depends on the **Q**-dependence of the quasi-elastic component: if it is **Q**-dependent and of the order of the instrumental resolution, contributions to MSDs extracted by slopes of linear fits are to be expected. On the other hand, if the quasi-elastic component is **Q**-independent in the investigated **Q**-range, one may focus on Gaussian motions. In this case, even though not affecting MSDs, the measured elastic intensities may be altered, as was shown in ''Protein powders hydrated in H_2O and D_2O'' section.

Conclusions

We have calculated the effect of diffusive motions on the elastic-window intensity for several scattering functions as a function of instrumental energy resolution and **Q**-range and interpreted experimental data from D_2O- and H_2O-hydrated protein powders. A criterion to classify diffusive motions was introduced, depending on the ratio of the widths of the diffusion scattering function and the instrumental energy resolution, as well as its variation as a function of **Q**. When both widths differ by at least one order of magnitude in a given **Q**-range, the influence of continuous translational diffusion is small on MSDs extracted from the corresponding elastic intensity. In contrast, when the widths are of the same order and the width of the diffusive scattering function varies with **Q**, MSDs extracted from elastic intensities are affected by diffusion.

Macromolecules in solution: we have shown that it is possible to focus specifically on intramolecular motions of macromolecules in solution when two conditions are fulfilled. (1) The width of the instrumental energy resolution has to differ by at least two orders of magnitude from the widths of the scattering functions associated with both the macromolecular as well as the solvent diffusion in the **Q**-range of interest. (2) The **Q**-values have to be chosen as large as possible without transgressing the validity of the Gaussian approximation for the intramolecular motions. Provided that both conditions are fulfilled, MSDs extracted by linear fits in Guinier plots represent intramolecular dynamics and experiments can be carried out both in D_2O and in H_2O. In all other cases, the diffusive motions ''contaminate'' MSDs extracted from IENS experiments.

Hydrated macromolecular powders: in H_2O-hydrated macromolecular powders, hydration water motions are more difficult to separate from intramolecular motions, mainly due to the fact that hydration water motions are reduced with respect to bulk water. Provided that the diffusion scattering function is independent of **Q** in a given range, intramolecular Gaussian motions can be extracted. However, changes in the absolute value of the measured elastic intensity are to be expected when using H_2O as hydration with respect to D_2O and care has to be taken in data interpretation.

Acknowledgements The author wishes to thank Dr. Giuseppe Zaccai and Prof. Marc Bée for their critical reading of the manuscript and helpful comments.

References

Becker T, Smith J (2003) Energy resolution and dynamical heterogeneity effects on elastic incoherent neutron scattering from molecular systems. Phys Rev E 67:021904 1–8

Bée M (1988) Quasielastic neutron scattering. Hilger, Bristol, UK

Bellissent-Funel MC (2004) Status of experiments probing the dynamics of water in confinement. Eur Phys J E 12:83–92

Bellissent-Funel MC, Zanotti JM, Chen SH (1996) Slow dynamics of water molecules on the surface of a globular protein. Faraday Discuss 103:281–294

Bon C, Dianoux AJ, Ferrand M, Lehmann MS (2002) A model for water motion in crystals of lysozyme based on an incoherent quasielastic neutron scattering study. Biophys J 83:1578–1588

Boutin H, Yip S (1968) Molecular spectroscopy with neutrons. MIT Press, Cambridge, Mass

Creighton T (1993) Proteins: structures and molecular properties. Freeman, New York

Dellerue S, Petrescu A-J, Smith JC, Bellissent-Funel M-C (2001) Radially softening diffusive motions in a globular protein. Biophys J 81:1666–1676

Doster W, Cusack S (1990) Temperature dependence of the low frequency dynamics of myoglobin. Measurement of the vibrational frequency distribution by inelastic neutron scattering. Biophys J 58:243–251

Doster W, Cusack S, Petry W (1989) Dynamical transition of myoglobin revealed by inelastic neutron scattering. Nature 337:754–756

Doster W, Diehl M, Gebhardt R, Lechner RE, Pieper J (2003) TOF-elastic resolution spectroscopy: time domain analysis of weakly scattering (biological) samples. Chem Phys 292:487–494

Dwyer JD, Bloomfield VA (1993) Brownian dynamics simulations of probe and self-diffusion in concentrated protein and DNA solutions. Biophys J 65:1810–1816

Ellis RJ (2001) Macromolecular crowding: an important but neglected aspect of the intracellular environment. Curr Opin Struct Biol 11:114–119

Ferrand M, Dianoux J, Petry W, Zaccai G (1993) Thermal motions and function of bacteriorhodopsin in purple membranes: effects of temperature and hydration studied by neutron scattering. Proc Natl Acad Sci USA 90:9668–9672

Fitter J, Lechner RE, Büldt G, Dencher NA (1996) Internal molecular motions of bacteriorhodopsin: hydration-induced flexibility studied by quasielastic incoherent neutron scattering using oriented purple membranes. Proc Natl Acad Sci USA 93:7600–7605

Frauenfelder H, Petsko GA, Tsernoglou D (1979) Temperature-dependent X-ray diffraction as a probe of protein structural dynamics. Nature 280:558–563

Frick B, Farago B (2002) Neutron spectroscopy by time-of-flight, backscattering and spin-echo techniques. In: Pike E, Sabatier P (eds) Scattering. Scattering and inverse scattering in pure and applied science. Academic Press, London, pp 1209–1241

Gabel F, Bicout D, Lehnert U, Tehei M, Weik M, Zaccai G (2002) Protein dynamics studied by neutron scattering. Q Rev Biophys 35:327–367

Gabel F, Weik M, Doctor BP, Saxena A, Fournier D, Brochier L, Renault F, Masson P, Silman I, Zaccai G (2004) The influence of solvent composition on global dynamics of human butyrylcholinesterase powders: a neutron scattering study. Biophys J 86:3152–3165

Gradshteyn IS, Ryzhik IM (1965) Table of integrals, series, and products. Academic Press, New York

Guinier A, Fournet G (1955) Small angle scattering of X-rays. Wiley, New York

Kneller GR, Smith JC (1994) Liquid-like side-chain dynamics in myoglobin. J Mol Biol 242:181–185

Kollmar A, Alefeld B (1976) In: Moon RM (ed) Proceedings of the conference on neutron scattering, Gatlinburg, Tenn., USA. Natl. Techn. Info. Service, US Dept. of Commerce, Washington, p 330

Lipowsky R, Sackmann E (1995) Handbook of biological physics, vol 1A. Structure and dynamics of membranes. From cells to vesicles. Elsevier, Amsterdam

Paciaroni A, Cinelli S, Onori G (2002) Effect of the environment on the protein dynamical transition: a neutron scattering study. Biophys J 83:1157–1164

Pérez J, Zanotti JM, Durand D (1999) Evolution of the internal dynamics of two globular proteins from dry powder to solution. Biophys J 77:454–469

Réat V, Zaccai G, Ferrand M, Pfister C (1997) Functional dynamics in purple membranes. In: Cusack S, Büttner H, Ferrand M, Langan P, Timmins P (eds) Biological macromolecular dynamics. Adenine Press, Schenectady, pp 117–122

Réat V, Patzelt H, Pfister C, Ferrand M, Oesterhelt D, Zaccai G (1998) Dynamics of different functional parts of bacteriorhodopsin: H-^{2}H labelling and neutron scattering. Proc Natl Acad Sci USA 95:4970–4975

Sears VF (1984) Thermal neutron scattering lengths and cross sections for condensed-matter research. Chalk River Nuclear Laboratories. Chalk River, Canada

Settles M, Doster W (1996) Anomalous diffusion of adsorbed water: a neutron scattering study of hydrated myoglobin. Faraday Discuss 103:269–279

Smith J (1991) Protein dynamics: comparison of simulations with inelastic neutron scattering experiments. Q Rev Biophys 24:227–291

Tehei M, Madern D, Pfister C, Zaccai G (2001) Fast dynamics of halophilic malate dehydrogenase and bovine serum albumin measured by neutron scattering under various solvent conditions influencing protein stability. Proc Natl Acad Sci USA 98:14356–14361

Tehei M, Franzetti B, Madern D, Ginzburg M, Ginzburg BZ, Giudici-Orticoni MT, Bruschi M, Zaccai G (2004) Adaptation to extreme environments: macromolecular dynamics in bacteria compared in vivo by neutron scattering. EMBO Rep 5:66–70

Teixeira J, Bellissent-Funel M-C, Chen SH, Dianoux J (1985) Experimental determination of the nature of diffusive motions of water molecules at low temperatures. Phys Rev A 31:1913–1917

Van Hove L (1954) Correlations in space and time and Born approximation scattering in systems of interacting particles. Phys Rev 95:249–259

Vineyard GH (1958) Scattering of slow neutrons by a liquid. Phys Rev 110:999–1010

Volino F, Dianoux J (1980) Neutron incoherent scattering function for diffusion in a potential of spherical symmetry: general information and application to diffusion inside a sphere. J Mol Phys 41:271–279

Volino F, Dianoux AJ, Lechner RE, Hervet H (1975) End chain motion in the solid phase of TTBA. J Phys T36 Suppl Colloq C1–C3, C1 83–88

Weast RC (ed) (1975) Handbook of chemistry and physics. CRC Press, Cleveland, Ohio